Electron-spectroscopy study of the semiconductor-metal transition in $La_{1-x}Sr_xCoO_3$

A. Chainani, M. Mathew, and D. D. Sarma
Solid State and Structural Chemistry Unit, Indian Institute of Science, Bangalore 560 012, India
(Received 2 April 1992; revised manuscript received 13 July 1992)

A study of the semiconductor-metal transition in the series $La_{1-x}Sr_xCoO_3$, $x=0.0$–0.4, using electron-spectroscopy techniques is presented. The results show that the ground state of $LaCoO_3$ has strongly mixed character. From the experiments we estimate the on-site Coulomb correlation energies U_{dd} and U_{pp} to be 3.4 and 6.7 eV, respectively, while the (pd_σ) interaction strength is 2.2 eV. A comparison of the experiment with the results of a model many-body cluster calculation for the Co $2p$ spectra indicates a low-spin state of Co in $LaCoO_3$. The band gap of $LaCoO_3$ is estimated to be about 0.6 eV from ultraviolet photoemission spectroscopy and bremsstrahlung isochromat spectroscopy measurements. The semiconductor-metal transition results from overlap of doped hole states with the valence band for $x \geq 0.2$.

INTRODUCTION

There has been a recent surge of activity in understanding the electronic structure of $3d$ transition-metal oxides in general and the metal-insulator transition in oxides in particular, following the discovery[1] of high temperature superconductivity in oxides. However, the challenge of understanding transition-metal oxides such as NiO, CoO, and V_2O_3 was recognized very early,[2] when the inadequacies of the one-electron picture became apparent. In fact, the varied properties of the transition-metal compounds and their oxides stem from their complex ground states. As estimated from calculations[3] and electron-spectroscopy studies,[4] the on-site Coulomb correlation energy is known to be large for the late transition metals and their compounds. Also, the charge-transfer energy, the exchange interaction, the crystal-field splitting, and the intersite hybridization are more often than not of comparable magnitude. Specifically for Co-oxide systems, recent estimates[5] from calculations for x-ray photoemission (xp) valence-band spectra have put the value of the on-site correlation energy, U_{dd} to be 5.3 eV for CoO and 3.5 eV for $LiCoO_2$. For the case of CoO, it has been shown by angle-resolved photoemission spectroscopy[6] that the $3d$ states have a dispersion much smaller than that obtained by density-functional band calculations and indicate the importance of correlation effects which are neglected in the one-electron picture. In spite of this evidence, however, in a recent spectroscopic study[7] of $LaCoO_3$ using x-ray absorption spectroscopy at the Co K edge and ultraviolet photoemission spectroscopy (UPS) as a function of temperature, Thornton, Owen, and Diakun have put forward an essentially independent particle model to explain the semiconductor-metal transition in $LaCoO_3$; it is suggested[7] that the high temperature metallic phase comes about due to the overlap of the primarily Co $3d$ derived π^* (t_{2g}) and empty σ^* (e_g) bands. Their proposal is a modification of the earlier empirical model due to Goodenough[8] and the authors conclude that strong correlations need not be invoked, their data being consistent with a one-electron picture for the electronic structure of $LaCoO_3$. The family of perovskite compounds $La_{1-x}Sr_xCoO_3$ has been extensively studied[7–12] for their interesting properties related to the semiconductor-metal transition as a function both of temperature at $x=0.0$ and of doping concentration, x. It is believed that the undoped $LaCoO_3$ exhibits a spin-state transition[10] in the semiconducting phase at low temperatures and becomes metallic above 750 K.[11] In the Sr doped system, $La_{1-x}Sr_xCoO_3$, the samples show itinerant ferromagnetism[12] for compositions of $x \geq 0.2$. While $La_{1-x}Sr_xCoO_3$ becomes metallic with Sr doping as in $La_{2-x}Sr_xCuO_4$, there are several important differences between the two systems. While the undoped La_2CuO_4 is an antiferromagnet with $T_n=250$ K (Ref. 13), $LaCoO_3$ does not exhibit magnetic ordering down to 4 K as determined by neutron diffraction data.[14] Magnetic susceptibility data have instead been interpreted as exhibiting a spin-state transition over a wide temperature range (70–150 K). On Sr doping, $La_{2-x}Sr_xCuO_4$ rapidly loses the magnetic order, while retaining antiferromagnetic correlations, before the system becomes metallic.[15] In contrast, $La_{1-x}Sr_xCoO_3$ becomes ferromagnetic[9] with T_c larger than 50 K for small doping of Sr ($x=0.1$), even in the insulating state. The T_c in fact increases with Sr content in this series. While the ground state of La_2CuO_4 is reasonably well described in terms of a charge-transfer insulator[15,16] with a strongly mixed-valent ground state, the description of the ground state of $LaCoO_3$ is not yet established. However, one would normally expect the U_{dd} to decrease and the bare charge-transfer energy Δ to increase for the transition metals with lower atomic number; this should somewhat shift the description of the electronic structure of $LaCoO_3$ towards the Mott-Hubbard insulator region in terms of the Zaanen-Sawatzky-Allen phase diagram.[17] On the other hand, the formally trivalent state of the cobalt atom in $LaCoO_3$ compared to the divalent state of copper in La_2CuO_4 may decrease the Δ value. The description of $LaCoO_3$ by Thornton, Tofield, and Williams would categorize it as a normal band insulator, where the gap opens up due to

band-structure effects or a Mott-Hubbard insulator, in contrast to the charge-transfer nature of La_2CuO_4, since the lowest energy charge excitation in this description involves a π^* (t_{2g} derived) to σ^* (e_g derived) excitation.

While it is quite clear that electron-spectroscopy techniques can provide important microscopic information concerning the electronic structure of these compounds few studies have been carried out on these systems. There have been studies[7,19,20] on $LaCoO_3$ using x-ray absorption at the Co K edge, x-ray and ultraviolet photoemission measurements on the valence-band and core-level XPS of the O 1s and Co 2p levels, but there are no electron-spectroscopy studies across the semiconductor to metal transition as a function of doping except for a report[18] of the valence-band XPS data in the semiconducting and metallic phases. Moreover, the unoccupied part of the density of states (DOS) has not been probed yet, even for $LaCoO_3$. Similarly Auger spectroscopic investigations have not been reported so far on these compounds. Thus we have carried out detailed investigations of the DOS using both XPS and UPS for the occupied part as well as bremsstrahlung isochromat (BI) spectroscopy for the unoccupied part for this series of compounds, providing information concerning the metal-insulator transition as a function of x or Sr doping. We have employed Auger electron spectroscopy (AES) to estimate the Coulomb correlation strengths, U_{dd} and U_{pp} in the Co 3d and oxygen 2p manifolds in this series of compounds. It is found that there are large and comparable Coulomb repulsions, U_{dd} and U_{pp}, within the Co 3d and O 2p states ensuring that a single particle description of these compounds is not realistic. We make use of x-ray photoemission spectra at the Co 2p core levels in conjunction with model Hamiltonian calculations to extract estimates of the hybridization strength between Co 3d and oxygen 2p states, as well as of the bare charge-transfer energies. These estimates provide a description of the ground states of $LaCoO_3$ as intermediate between the charge-transfer and the Mott-Hubbard insulator.

EXPERIMENT

The compounds $La_{1-x}Sr_xCoO_3$ ($x=0.0$ 0.1, 0.2, 0.3, and 0.4) were prepared by the ceramic method, using La_2O_3, $CoC_2O_4\cdot 2H_2O$ and $SrCO_3$ in the required proportions, grinding it together and heating it at 1073 K for a day. This was followed by grinding, pelletizing and heating at 1223 K for two days, for a minimum of three cycles. The compounds are known[9] to have the rhombohedrally distorted perovskite structure, with the distortion decreasing for increasing x and this was confirmed by powder x-ray diffraction. The oxygen content of the samples was determined using electrochemical titrations and it was found that the oxygen stoichiometry was slightly deficient for $x \geq 0.2$. The measured stoichiometry for various x values are as follows: $LaCoO_{2.99}$, $La_{0.9}Sr_{0.1}CoO_{2.98}$, $La_{0.8}Sr_{0.2}CoO_{2.95}$, $La_{0.7}Sr_{0.3}CoO_{2.95}$, $La_{0.6}Sr_{0.4}CoO_{2.95}$. The resistivity of the samples below room temperature (20–300 K) confirmed[9,12] that for $x \geq 0.2$, the samples had a positive temperature coefficient of resistivity.

The XPS, UPS, and BIS measurements were carried out on a combined XPS-UPS-BIS electron spectrometer of VSW Scientific Instruments Ltd., Manchester. All the experiments were done on well-sintered pellets at a vacuum of about $7-8\times10^{-10}$ torr. The XPS measurements were done using a Mg$K\alpha$ source with a total resolution of about 0.8 eV. The UPS data were collected with a He I radiation from a discharge lamp with a resolution of 140 meV. The BIS data were acquired using an incident electron beam current of 120 μA at a fixed photon energy of 1486.6 eV. The resolution in this case was about 0.8 eV. The spectrometer Fermi level was checked for each sample using the copper stub on which the sample was mounted. No surface charging was observed for the semiconducting samples. The cleanliness of the sample surface was ensured by *in situ* scraping of the surface with an alumina file. The O 1s XP spectra showed a higher binding energy shoulder as reported earlier by Veal and Lam.[19] The sample surface was scraped until this feature showed no further decrease in intensity. We have also checked the oxygen 1s spectra with the samples at a low temperature (about 80 K); this procedure is known[21] to produce cleaner surfaces in the case of La_2CuO_4 and other high-temperature cuprate superconductors. However, in the present series of compounds temperature was found to have insignificant effects. The C 1s signal due to carbonate impurity was negligible in all the samples. A check for possible charging effects as well as degrading of the sample surface during BIS measurements were done by varying the electron current and by moving the electron beam spot to a new part of the sample surface for each individual scan.

RESULTS AND DISCUSSION

In Fig. 1 we show the x-ray photoelectron spectra of the valence-band regions in $La_{1-x}Sr_xCoO_3$ with $x=0.0$, 0.1, 0.2, 0.3, and 0.4. Undoped $LaCoO_3$ exhibits a sharp feature close to E_F at about 1.0 eV binding energy followed by a weak feature at about 3.3 eV binding energy.

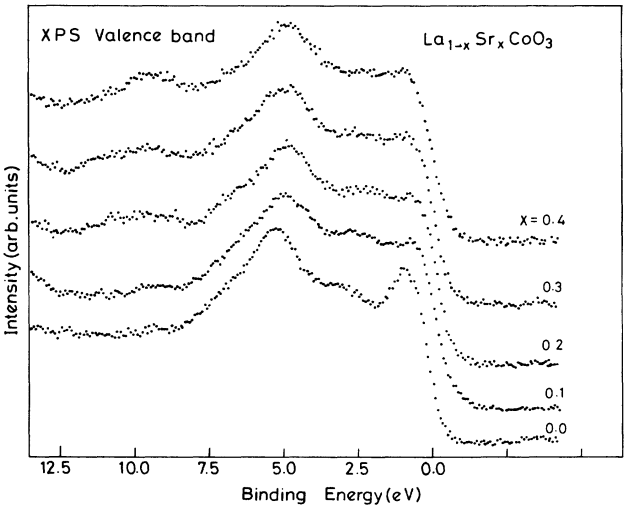

FIG. 1. The XPS valence band of $La_{1-x}Sr_xCoO_3$ ($x=0.0$–0.4) using Mg$K\alpha$ source.

The most intense peak in the spectrum appears at about 5.3 eV below E_F. The position of the leading peak close to E_F leads to a finite intensity at E_F in the spectrum due to resolution broadening in the case of insulating $LaCoO_3$. Thus E_F appears to be pinned very close to the top of the valence band in this case. On doping Sr in place of La in the compound, several changes are noticeable in the spectra (Fig. 1). A broad and weak feature appears to grow systematically at about 10.0 eV binding energy. This feature is due to the $\alpha_{3,4}$ satellite of the Sr $4p$ emission at higher binding energy. Besides this artifact, all the spectral features are found to be distinctly broadened on Sr doping (Fig. 1). This is easily seen by the near absence of the dip in the spectral intensity at about 1.9 eV below E_F of the $LaCoO_3$ spectrum on Sr doping. The peak at 5.3 eV binding energy is also found to broaden considerably. We also find that the peak at 5.3 eV below E_F in $LaCoO_3$ shifts to lower binding energy by approximately 0.6 eV on doping with Sr. Most importantly, we find that there is a small but systematic increase of the spectral intensity at E_F with increasing x (or Sr content). While we do not observe a clear emergence of a Fermi cutoff in the metallic cases ($x \geq 0.2$) as distinct from the insulating ones, the increase in the spectral intensity at E_F must be related to the changes in the conducting properties of these samples.

In order to see the changes in the valence-band spectral features with higher resolution as well as to understand the nature of the various states, we have recorded the ultraviolet photoelectron spectra of $La_{1-x}Sr_xCoO_3$ series using He I radiation. The UP spectra are shown in Fig. 2(a). The spectra in Fig. 2(a) show features at 1.2, 2.8, and 5.7 eV below E_F. Once again we find a shift of the peak 5.7 eV below E_F in $LaCoO_3$ by 0.6 eV to lower binding energy on Sr doping. It is interesting to note that the spectral feature nearest to E_F in these compounds has considerably higher relative intensity in x-ray photoemission spectra (Fig. 1) compared to the uv photoemission spectra (Fig. 2). This fact suggests that this feature has strong Co $3d$ admixture, as the cross section for Co $3d$ emission relative to oxygen $2p$ emission is considerably larger at the x-ray energies.[22]

A close inspection near E_F in Fig. 2(b) reveals that there is a small gap (about 0.1–0.2 eV) between the onset of spectral intensity and E_F in the case of $LaCoO_3$, in agreement with its insulating property. On doping with Sr, the spectral intensity becomes finite at E_F; however, this intensity remains very small for all the samples. Thus it appears that the low DOS tail of the doped hole states overlap the Fermi level making the system metallic with Sr doping. Similar to the XP spectra, an overall broadening of the spectral features is also visible in the UP spectra (Fig. 2) on doping with Sr.

Since substituting Sr^{2+} in place of La^{3+} introduces holes in the system, we expect to see more pronounced modifications of the spectral features of the unoccupied part of the DOS on doping. Thus we have probed the unoccupied DOS of these compounds using bremsstrahlung isochromat spectroscopy. The BI spectra of these compounds are shown in Fig. 3(a). The intense peak at about 9.0 eV above E_F is due to La $4f$ states as is also seen[23] in La_2CuO_4. The peak at about 3.0 eV above E_F in $LaCoO_3$ corresponds to transitions into the upper Hubbard band formed from hybridization of Co $3d$ states with oxygen $2p$ states. This peak shows systematic changes on doping, as shown in Fig. 3(b) in an expanded scale. Figure 3(b) clearly shows that the intensity of the peak close to E_F increases progressively with Sr doping representing the spectral features of the hole doped states. Since this spectroscopy is primarily sensitive to Co $3d$ states compared to oxygen $2p$ states, it is reasonable to assume that the doped hole states have substantial

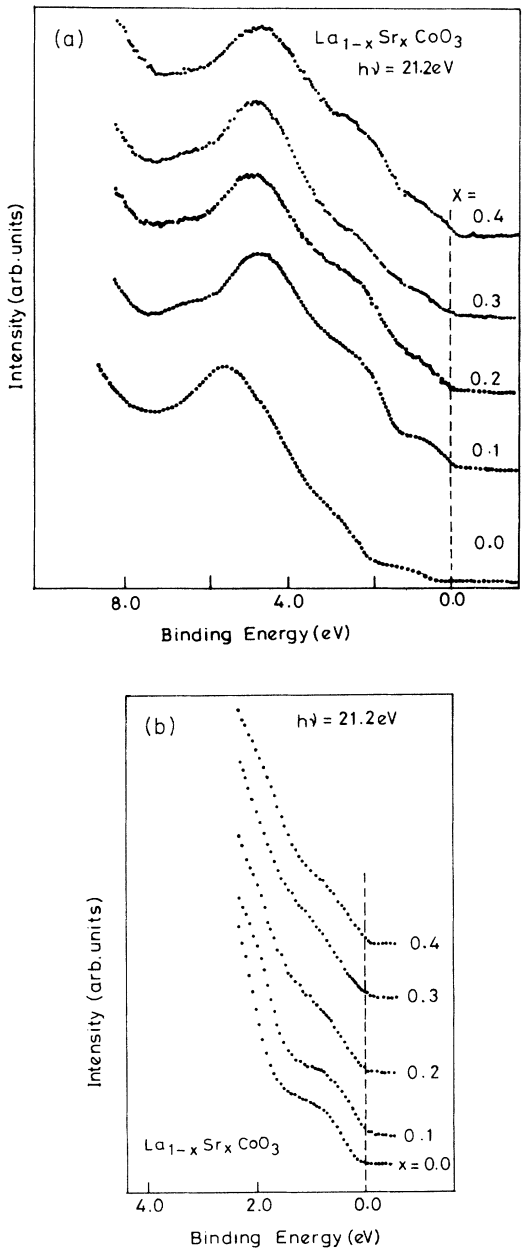

FIG. 2. (a). The valence-band spectra of $La_{1-x}Sr_xCoO_3$ ($x=0.0$–0.4) obtained using He I radiation source with the peak at 5.3 eV normalized. (b). Details of the spectra near E_F with improved signal-to-noise ratio drawn relative to the Fermi energy on an expanded scale.

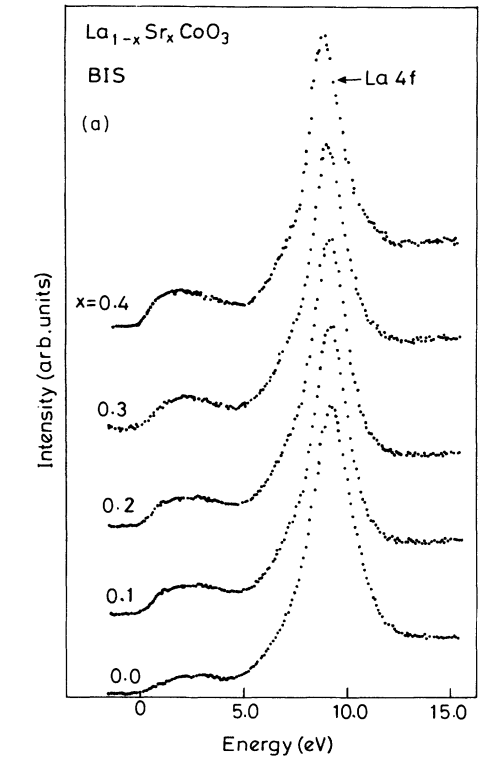

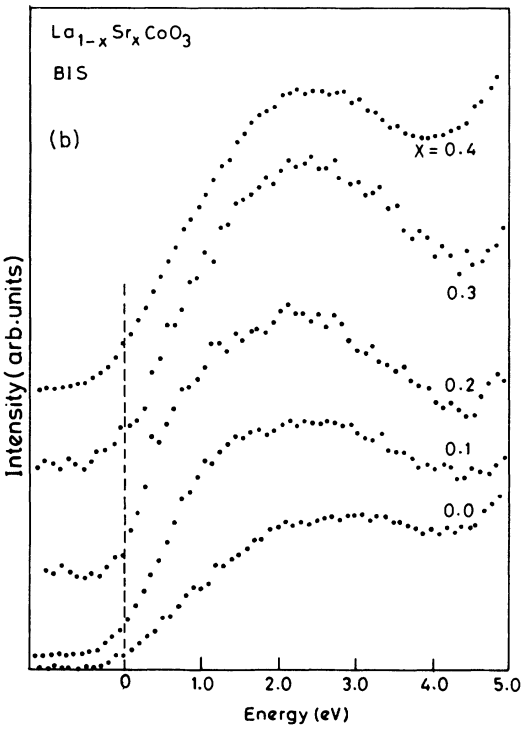

FIG. 3. (a). The bremsstrahlung isochromat spectra for the series $La_{1-x}Sr_xCoO_3$ with the spectra normalized at the La $4f$ peak. (b). The near E_F BI spectra with improved signal-to-noise ratio drawn relative to the Fermi energy on an expanded scale.

Co $3d$ character.

The increased intensity due to the doped states also leads to an increase of the spectral intensity at the Fermi energy [Fig. 3(b)]. The spectral features suggest that the low energy weak intensity tail of the doped states overlap E_F in the Sr-doped compounds, as already suggested on the basis of XP and UP spectra. For $LaCoO_3$ we estimate a gap of about 0.4 eV between E_F and the upper Hubbard band. Together with the gap in the occupied part, we estimate a conductivity gap of 0.6 ± 0.2 eV for $LaCoO_3$. While the low temperature resistivity data[9,12] suggest a gap of about 0.2 eV for $LaCoO_3$, the high temperature resistivity indicates[11] a gap of 0.5 eV, in agreement with the present estimate. It appears that the low temperature resistivity data may be dominated by impurity and/or defect induced states, as is known to happen in many of these oxide materials.

In order to estimate the Coulomb correlation strength in these compounds, we have used Auger electron spectroscopy. The Auger electron (AE) spectra of Co $L_{2,3}$-$M_{4,5}M_{4,5}$ transition in $La_{1-x}Sr_xCoO_3$ are shown in Fig. 4 and AE spectra of O K-$L_{2,3}L_{2,3}$ in Fig. 5. The spectral features do not significantly change with Sr doping, indicating very similar Coulomb correlation strengths, U_{dd} and U_{pp}, in these compounds. In order to extract a quantitative estimate of U_{dd}, we compare the Co L_3-$M_{4,5}M_{4,5}$ spectrum of $LaCoO_3$ with the self-convoluted DOS after aligning them to the respective Fermi energies in Fig. 6(a). In order to obtain the self-convoluted DOS, we adopt the XP spectrum of the valence band in $LaCoO_3$. Since the peak at 5.3 eV below E_F is primarily due to oxygen $2p$ emission, we exclude it from the calculation of the self-convoluted DOS as shown in the inset of Fig. 6(a) by a dashed line. This procedure leads to a very good description of the high-energy features in the Auger spectrum as is evident in Fig. 6(a), identifying the shoulder in the AE spectrum at 775.0 eV kinetic energy to be due to transitions into the uncorrelated two-hole final state. The main peak in AE spectrum is then due to a correlated two hole final state. Thus the energy difference (3.4 eV) between these two

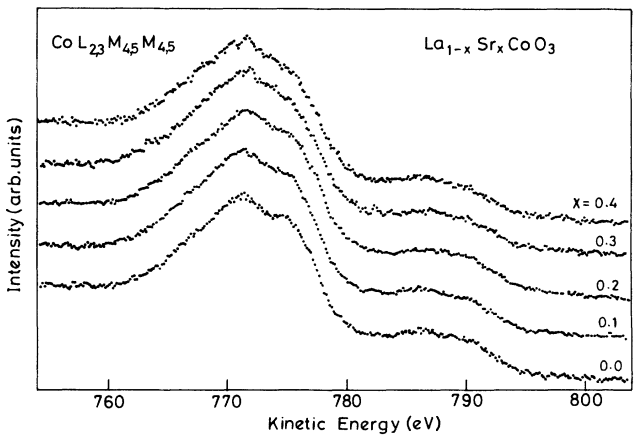

FIG. 4. The Co $L_{2,3}$-$M_{4,5}M_{4,5}$ Auger spectra of $La_{1-x}Sr_xCoO_3$ ($x=0.0$–0.4).

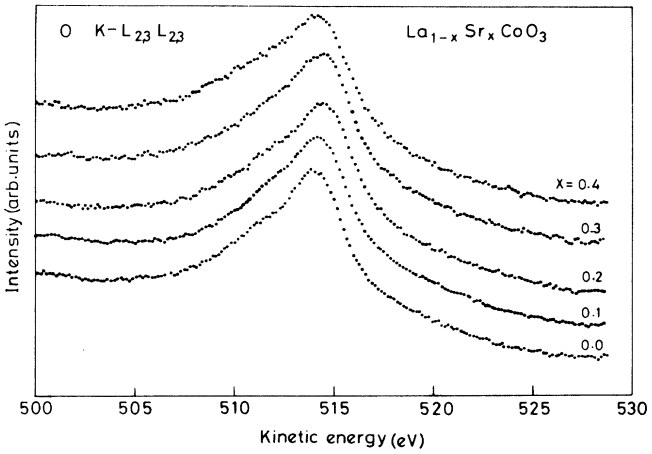

FIG. 5. The O K-$L_{2,3}L_{2,3}$ Auger spectra of the series $La_{1-x}Sr_xCoO_3$ ($x=0.0$–0.4).

features provides us with an estimate of U_{dd}. Similarly we compare the self-convoluted spectrum of the total valence band of $LaCoO_3$ with the oxygen K-$L_{2,3}L_{2,3}$ Auger spectrum in Fig. 6(b). This comparison provides an estimate of U_{pp} to be 6.7 eV, as shown in the figure. The estimate of U_{pp} is in agreement with the estimates of the same quantity from other oxide materials.[24] Moreover, the present estimate of U_{dd} is in very good agreement with the U_{dd} value deduced[5] for $LiCoO_2$ which is another formally Co^{3+} compound.

In Fig. 7 we show the Co $2p$ spectra from these compounds. The most intense peak at 780 eV binding energy is due to the Co $2p_3$ main peak and the peak at 764.5 eV is due to the Co $2p_{1/2}$ main peak. The binding energy of these peaks does not shift within the experimental accuracy on doping with Sr indicating that there is no appreciable shift in the position of the Fermi level in this series of compounds. However, we find that there are systematic changes in the full widths at half maxima (FWHM's) of these peaks. The FWHM's for the $2p_{3/2}$ peak are 3.8 eV ($x=0.0$), 4.8 eV ($x=0.1$), 4.5 eV ($x=0.2$), 4.2 eV ($x=0.3$) and 4.0 eV ($x=0.4$). From this we find that the FWHM of the $LaCoO_3$ $2p_{3/2}$ peak (3.8 eV) increases substantially for $La_{0.9}Sr_{0.1}CoO_3$ to 4.8 eV. On further doping the FWHM becomes smaller for $x \geq 0.2$. A similar trend is also seen in the $2p_{1/2}$ spectra. We believe that Sr doping introduces local high-spin states near the doping sites in the insulating phase, leading to small shifts in the binding energies of the Co core levels. This inhomogeneous effect manifests itself as a broadening of the core-level spectrum for the $x=0.1$ insulating sample (see text later). On further doping the compounds become metallic, leading to the same situation at every site, explaining the reduction in the FWHM of the Co $2p$ spectra for $x \geq 0.2$.

In all the spectra shown in Fig. 7, a weak satellite feature can be seen at about 10 eV higher binding energy from the main peak. It is well known[4,25] that such satellites appear in core-level spectra of a wide variety of compounds arising from an interplay of hybridization and correlation effects, and thus provides a means to obtain estimates of these important interaction strengths that determine the electronic structure. In order to do so, we calculate the core-level spectra within the cluster approximation using an octahedral $(CoO_6)^{9-}$ cluster both for the low-spin and high-spin configurations. The basis states as well as the Hamiltonian matrix elements for both these spin configurations are given in Table I. Since a large number of parameters appear in the calculation, we have fixed some of the interaction strengths. For ex-

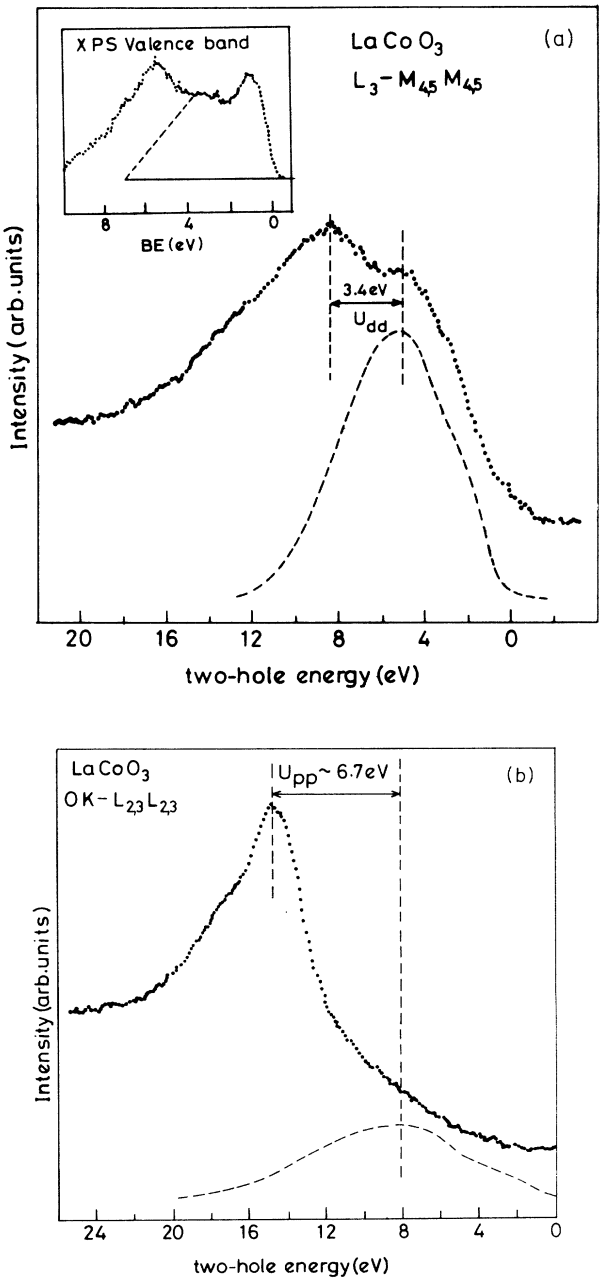

FIG. 6. (a). The self-convoluted DOS along with the Co L_3-$M_{4,5}M_{4,5}$ Auger spectrum of $LaCoO_3$, with their respective Fermi energies aligned. Inset shows the part of the XPS valence band used to calculate the self-convoluted DOS. (b). The O K-$L_{2,3}L_{2,3}$ Auger spectrum drawn with the self-convoluted DOS of the total valence band.

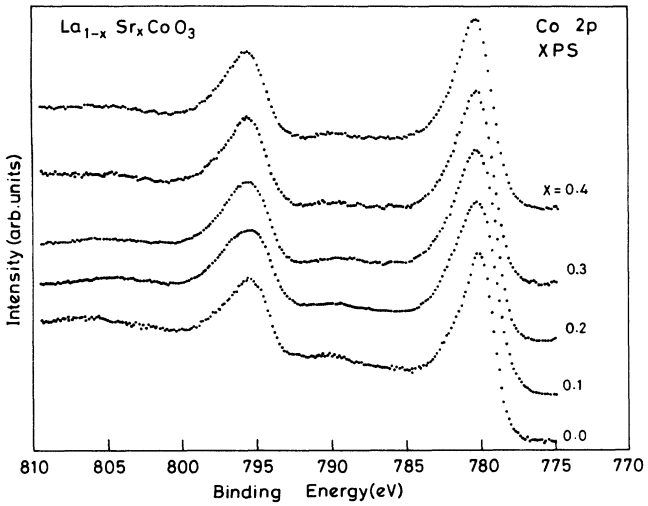

FIG. 7. The Co $2p$ x-ray photoemission spectra for $La_{1-x}Sr_xCoO_3$ ($x=0.0$–0.4).

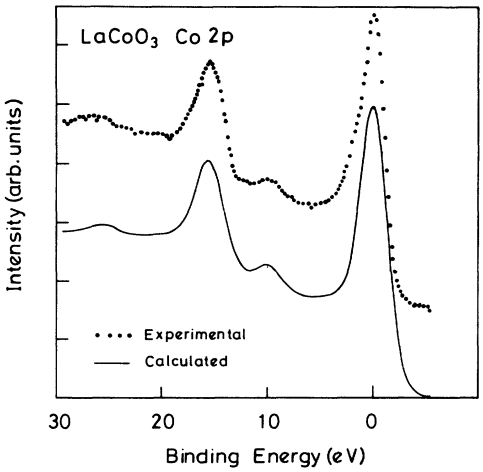

FIG. 8. The calculated Co $2p$ photoemission spectrum for the low-spin configuration of Co in a $(CoO_6)^{9-}$ cluster, compared with the experimental curve. The $\alpha_{3,4}$ satellites have been removed from the experimental spectrum.

ample, U_{dd} is fixed at the experimentally obtained value of 3.4 eV. The $2p$ core hole-valence hole repulsion strength, U_{dc}, is taken approximately as $U_{dc}=U_{dd}\times 1.1$. The bare crystal-field splitting of the Co $3d$ into t_{2g} and e_g levels is taken as 1.0 eV and the exchange energy J is taken to be 0.5 eV in order to make the energy difference between the high-spin and low-spin ionic states small. The bare energy difference between the symmetry-adapted oxygen t_{2g} and e_g states was estimated to be 1.5 eV from multiple-scattering $X\alpha$ calculations[26] on the $(CoO_6)^{9-}$ cluster. The hybridization strength between the Co $3d$ t_{2g} and oxygen symmetry-adapted t_{2g} state was taken[5] to be half of that between the e_g states. This approach leaves two adjustable parameters, the bare charge-transfer energy and the Co $3d$ e_g hybridization strength t with the corresponding oxygen states, for fitting the calculated spectra to the experimental one. We find that the high-spin configuration is not at all compatible with the experimental spectra, whereas the low-spin configuration simulates the spectrum remarkably well with $t=3.8\pm0.2$ eV. This corresponds to a $(pd\sigma)$ interaction strength of 2.2 ± 0.1 eV, which is close to the value of $(pd\sigma)$ obtained[5] for $LiCoO_2$, which is another Co^{3+} with octahedral oxygen coordination around Co. We show the comparison of the experimental spectrum with the calculated one for the low-spin configuration with $t=3.8$ eV and $\Delta=4.0$ eV in Fig. 8. For the purpose of this comparison we have removed the $\alpha_{3,4}$ component from the experimental spectrum. The calculated spectrum was broadened by a Gaussian of width 2.8 eV representing the multiplet spread and resolution broadening. An integral background was incorporated in the calculated spectrum. The spin-orbit doublet was incorporated by shifting the calculated spectrum by the experimental spin-orbit splitting (15.5 eV) and by reducing the intensity to half. Moreover, a small additional broadening of the $2p_{1/2}$ related structure due to the extra Coster-Kronig decay channel for the $2p_{1/2}$ core hole was incorporated by broadening of this part of the spectrum

TABLE I. Basis states and Hamiltonian matrix elements for the low-spin and high-spin configurations of $(CoO_6)^{9-}$ cluster. For the low spin case, $H(1,2)=H(1,4)=H(2,3)=H(2,6)=H(3,8)=H(4,5)=H(4,6)=H(5,7)=H(6,7)=H(6,8)=H(7,9)=H(8,9)=\sqrt{2}t$, and all other matrix elements are zero. For the high-spin case, $H(1,2)=H(2,3)=H(4,6)=H(5,7)=H(6,8)=H(7,9)=\sqrt{2}t_1$, $H(1,4)=H(2,6)=H(3,8)=H(4,5)=H(6,7)=H(8,9)=\sqrt{2}t_2$, and all other matrix elements are zero. And also for the high-spin case, $Q=q_1+q_2$ where q_1 is the crystal-field splitting in the Co $3d$ states and q_2 is the oxygen $2p$ derived t_{2g}-e_g splitting due to oxygen-oxygen interaction.

Low-spin case	
$\phi_1=\lvert t_{2g\uparrow}^3 t_{2g\downarrow}^3 e_{g\uparrow}^0 e_{g\downarrow}^0\rangle$	$H(1,1)=0$
$\phi_2=\lvert t_{2g\uparrow}^3 t_{2g\downarrow}^3 e_{g\uparrow}^1 e_{g\downarrow}^0 \underline{L}_{\sigma\downarrow}^1\rangle$	$H(2,2)=\Delta$
$\phi_3=\lvert t_{2g\uparrow}^3 t_{2g\downarrow}^3 e_{g\uparrow}^2 e_{g\downarrow}^0 \underline{L}_{\sigma\downarrow}^2\rangle$	$H(3,3)=2\Delta+U_{dd}-J$
$\phi_4=\lvert t_{2g\uparrow}^3 t_{2g\downarrow}^3 e_{g\uparrow}^0 e_{g\downarrow}^1 \underline{L}_{\sigma\uparrow}^1\rangle$	$H(4,4)=H(2,2)$
$\phi_5=\lvert t_{2g\uparrow}^3 t_{2g\downarrow}^3 e_{g\uparrow}^0 e_{g\downarrow}^2 \underline{L}_{\sigma\uparrow}^2\rangle$	$H(5,5)=H(3,3)$
$\phi_6=\lvert t_{2g\uparrow}^3 t_{2g\downarrow}^3 e_{g\uparrow}^1 e_{g\downarrow}^1 \underline{L}_{\sigma\downarrow}^1 \underline{L}_{\sigma\uparrow}^1\rangle$	$H(6,6)=2\Delta+U_{dd}$
$\phi_7=\lvert t_{2g\uparrow}^3 t_{2g\downarrow}^3 e_{g\uparrow}^1 e_{g\downarrow}^2 \underline{L}_{\sigma\downarrow}^1 \underline{L}_{\sigma\uparrow}^2\rangle$	$H(7,7)=3\Delta+3U_{dd}-J$
$\phi_8=\lvert t_{2g\uparrow}^3 t_{2g\downarrow}^3 e_{g\uparrow}^2 e_{g\downarrow}^1 \underline{L}_{\sigma\downarrow}^2 \underline{L}_{\sigma\uparrow}^1\rangle$	$H(8,8)=H(7,7)$
$\phi_9=\lvert t_{2g\uparrow}^2 t_{2g\downarrow}^3 e_{g\uparrow}^2 e_{g\downarrow}^2 \underline{L}_{\sigma\downarrow}^2 \underline{L}_{\sigma\uparrow}^2\rangle$	$H(9,9)=4\Delta+6U_{dd}-2J$
High-spin case	
$\phi_1=\lvert t_{2g\uparrow}^3 t_{2g\downarrow}^1 e_{g\uparrow}^2 e_{g\downarrow}^0\rangle$	$H(1,1)=0$
$\phi_2=\lvert t_{2g\uparrow}^3 t_{2g\downarrow}^1 e_{g\uparrow}^2 e_{g\downarrow}^1 \underline{L}_{\sigma\uparrow}^1\rangle$	$H(2,2)=\Delta$
$\phi_3=\lvert t_{2g\uparrow}^3 t_{2g\downarrow}^1 e_{g\uparrow}^2 e_{g\downarrow}^2 \underline{L}_{\sigma\uparrow}^2\rangle$	$H(3,3)=2\Delta+U$
$\phi_4=\lvert t_{2g\uparrow}^3 t_{2g\downarrow}^2 e_{g\uparrow}^2 e_{g\downarrow}^0 \underline{L}_{\pi\uparrow}^1\rangle$	$H(4,4)=\Delta+Q$
$\phi_5=\lvert t_{2g\uparrow}^3 t_{2g\downarrow}^3 e_{g\uparrow}^2 e_{g\downarrow}^0 \underline{L}_{\pi\uparrow}^2\rangle$	$H(5,5)=2\Delta+2Q+U$
$\phi_6=\lvert t_{2g\uparrow}^3 t_{2g\downarrow}^2 e_{g\uparrow}^2 e_{g\downarrow}^1 \underline{L}_{\sigma\uparrow}^1 \underline{L}_{\pi\uparrow}^1\rangle$	$H(6,6)=2\Delta+Q+U$
$\phi_7=\lvert t_{2g\uparrow}^3 t_{2g\downarrow}^2 e_{g\uparrow}^2 e_{g\downarrow}^1 \underline{L}_{\sigma\uparrow}^1 \underline{L}_{\pi\uparrow}^2\rangle$	$H(7,7)=3\Delta+Q+3U$
$\phi_8=\lvert t_{2g\uparrow}^3+t_{2g\downarrow}^2 e_{g\uparrow}^2 e_{g\downarrow}^2 \underline{L}_{\sigma\uparrow}^2 \underline{L}_{\pi\uparrow}^1\rangle$	$H(8,8)=H(7,7)$
$\phi_9=\lvert t_{2g\uparrow}^2 t_{2g\downarrow}^3 e_{g\uparrow}^2 e_{g\downarrow}^2 \underline{L}_{\sigma\uparrow}^2 \underline{L}_{\pi\uparrow}^2\rangle$	$H(9,9)=4\Delta+2Q+6U$

with a Lorentzian ($\Gamma=0.4$ eV). The resulting calculated spectrum is a very good fit to the experimental spectrum, as is evident from Fig. 8. The main discrepancy between the experimental and the calculated spectra appears to be in the high binding energy side due to underestimation of the inelastic scattering background. We find that the hybridization strength t has to be in the range 3.8 ± 0.2 eV for a reasonable description of the spectra, independent of all other parameter values. In this sense the experimental spectrum provides a reasonably precise estimate of the hybridization strength. Interestingly enough, we find that the calculated spectral shape hardly depends on the charge-transfer excitation energy, Δ, and this parameter cannot be fixed at all from the core-level spectra. The spectral shape appears to be primarily determined by the presence of very large hybridization strength, providing the dominant energy scale in the problem. A similar observation has been made for $LiCoO_2$ recently.[5] If we assume that Δ will not be very different between the two Co^{3+} low-spin oxide systems ($LaCoO_3$ and $LiCoO_2$), having very similar local coordination around the Co ion, we find that the ground state of $LaCoO_3$ corresponds to a primarily low-spin configuration with $U_{dd}=3.4$ eV, $\Delta\sim4.0$ eV, and $t=3.8$ eV. The ground state with these parameter values turns out to be a very mixed state with 38.5% d^6, 45.4% $d^7\underline{L}$ and 14.5% $d^8\underline{L}^2$ characters. Such a ground state with $U/t\sim1$ and $\Delta/t\sim1$ place $LaCoO_3$ in the mixed character region between Mott-Hubbard, charge-transfer and covalent insulators in terms of the modified[27] Zaanen-Sawatzky Allen phase diagram.[17]

With the above-mentioned parameter values the doped hole state of $(CoO_6)^{8-}$ will have the lowest energy for high-spin Co^{4+} $3d^5$ ($t_{2g}^3e_g^2$) state; this state has an energy approximately 1 eV lower than those of the low-spin Co^{4+} (t_{2g}^5) state and the intermediate-spin Co^{4+} ($t_{2g}^4e_g^1$) state. Moreover, the high-spin $t_{2g}^3e_g^2$ state is approximately 4 eV lower in energy compared to the corresponding charge-transferred state $t_{2g}^4e_g^2\underline{L}_\pi^1$, $\underline{L}_\pi^1$ denoting a hole in the oxygen $2p$-derived t_{2g} symmetry-adapted state. The charge-transferred state corresponds to the situation where the doped hole resides at the oxygen sites. However, it should be noted that the large hybridization strength between the Co $3d$ and O $2p$ will admix these states appreciably. In fact, the energetics of the doped-hole state is very similar to that of the undoped $(CoO_6)^{9-}$ cluster where the low-spin $t_{2g}^6e_g^0$ state has an energy of 4 eV lower than that of the charge-transferred $t_{2g}^6e_g^1\underline{L}_\sigma^1$ state. However, the large hybridization strength coupled with the high degeneracy of the charge-transferred state ensures a 45% contribution to the ground state of the cluster in this case, compared to the 39% contribution coming from the $t_{2g}^6e_g^0$ state, as has already been pointed out. Similarly in the doped-hole case, we expect that a large weight of the doped hole will reside at the oxygen sites.

Magnetic measurements[9] support the suggestion made here that the hole doping leads to the formation of the high-spin state rather than the low-spin configuration. It has been reported[10] that the effective magnetic moment of Co^{3+} in $LaCoO_3$ is about 3.1 Bohr magnetons, in the temperature range of 150–400 K. For small doping of Sr ($x=0.05$) in $La_{1-x}Sr_xCoO_3$, the effective magnetic moment increases to about 4.5 Bohr magnetons, suggesting the formation of the high-spin state. This would also explain the strong changes observed in the spectral features in the XPS core level (Fig. 7) and valence band (Fig. 1) for the $x=0.1$ sample. In this insulating regime, the doped holes are still localized, transforming some of the local clusters to the high-spin states while the remaining ones are in the low-spin configuration. This leads to the observed marked broadening of the Co $2p$ spectrum (Fig. 7) as well as the changes in the valence-band spectrum (Fig. 1) for $x=0.1$ compared to the $x=0.0$ sample.

CONCLUSIONS

It is shown that $LaCoO_3$ is an insulator with an intrinsic conductivity gap of about 0.6 eV. Replacing La with Sr introduces hole states above the Fermi level with substantial Co $3d$ character. With increasing Sr content, these doped states broaden to overlap E_F making the material metallic for $x\geq0.2$ in $La_{1-x}Sr_xCoO_3$. The Coulomb correlation strength U_{dd} is estimated to be approximately 3.4 eV from the Auger spectra. Analysis of the core level provides an estimate of the hybridization strength between the Co $3d$ e_g state and the oxygen states to be about 3.8 eV. These parameter strengths place $LaCoO_3$ in the highly mixed character region between Mott-Hubbard, charge-transfer and covalent insulator phases. This indicates that the doped-hole states will have considerably mixed Co $3d$ and oxygen $2p$ characters in $La_{1-x}Sr_xCoO_3$.

ACKNOWLEDGMENTS

We thank Professor C. N. R. Rao for his support of this research. Financial support from the Department of Science and Technology and Department of Atomic Energy, Government of India are acknowledged. A. C. and M. M. thank the Council of Scientific and Industrial Research for financial support.

[1]J. G. Bednorz and K. A. Muller, Z. Phys. B **64**, 189 (1986).
[2]N. F. Mott, Proc. Phys. Soc. London, Ser. A **62**, 416 (1949).
[3]T. Bandyopadhyay and D. D. Sarma, Phys. Rev. B **39**, 3517 (1989).
[4]A. Fujimori, F. Minami, and S. Sugano, Phys. Rev. B **29**, 5225 (1984); G. A. Sawatzky and J. W. Allen, Phys. Rev. Lett. **53**, 2339 (1984).
[5]J. van Elp, J. L. Wieland, H. Eskes, P. Kuiper, G. A. Sawatzky, F. M. F. de Groot, and T. S. Turner, Phys. Rev. B **44**, 6090 (1991).
[6]Z-X Shen, C. K. Shih, O. Jepsen, W. E. Spicer, I. Lindau, and J. W. Allen, Phys. Rev. Lett. **64**, 2442 (1990).
[7]G. Thornton, I. W. Owen, and G. P. Diakun, J. Phys.: Condens. Mater **3**, 417 (1991).
[8]J. B. Goodenough, J. Phys. Chem. Solids **6**, 287 (1958).
[9]G. H. Jonker and V. H. Van Santen, Physica **19**, 120 (1953); P.

M. Raccah and J. B. Goodenough, J. Appl. Phys. **39**, 1209 (1968); J. B. Goodenough, in *Progress in Solid State Chemistry*, edited by H. Reiss (Pergamon, London, 1971), Vol. 5, 145.
[10]C. S. Naiman *et al.*, J. Appl. Phys. **36**, 1044 (1965); R. R. Heikes, R. C. Miller, and R. Mazelsky, Physica **30**, 1600 (1964).
[11]G. Thornton, B. C. Tofield, and D. E. Williams, Solid State Commun. **44**, 1213 (1982).
[12]V. G. Bhide, D. S. Rajoria, C. N. R. Rao, G. Rama Rao, and V. G. Jadhao, Phys. Rev. B **12**, 2832 (1972); V. G. Bhide, D. S. Rajoria, C. Rama Rao, and C. N. R. Rao, *ibid.* **6**, 1021 (1972).
[13]K. Sreedhar and C. N. R. Rao, Mater. Res. Bull. **25**, 1235 (1990).
[14]W. C. Koehler and E. O. Wollan, J. Phys. Chem. Solids **2**, 100 (1957).
[15]D. D. Sarma, Phys. Rev. B **37**, 7948 (1988).
[16]A. Fujimori *et al.*, Phys. Rev. B **35**, 8814 (1987); Z. Shen *et al.*, *ibid.* **36**, 8414 (1987).
[17]J. Zaanen, G. A. Sawatzky, and J. W. Allen, Phys. Rev. Lett. **55**, 418 (1985).
[18]G. Thornton, A. F. Orchard, and C. N. R. Rao, J. Phys. C **9**, 1991 (1976).
[19]B. W. Veal and D. J. Lam, J. Appl. Phys. **49**, 1461 (1978); D. J. Lam, B. W. Veal, and D. E. Ellis, Phys. Rev. B **22**, 5730 (1980).
[20]L. Richter, S. D. Bader, and M. B. Brodsky, Phys. Rev. B **22**, 3059 (1980).
[21]T. Takahashi *et al.*, Phys. Rev. B **37**, 9788 (1988).
[22]J. J. Yeh and I. Lindau, At. Data Nucl. Data Tables **32**, 1 (1985).
[23]Y. Gao, T. J. Wagener, J. H. Weaver, A. J. Arko, B. Flandermeyer, and D. W. Capone II, Phys. Rev. B **36**, 3971 (1987).
[24]D. van der Marel *et al.*, Phys. Rev. B **37**, 5136 (1988).
[25]O. Gunnarsson *et al.*, Phys. Rev. B **32**, 5499 (1985); D. D. Sarma *et al.*, Z. Phys. B **63**, 305 (1986).
[26]D. D. Sarma, A. K. Santra, and C. N. R. Rao (unpublished).
[27]D. D. Sarma, J. Solid State Chem. **88**, 45 (1990); D. D. Sarma *et al.*, Pramana-J. Phys. **38**, L531 (1992).